Open access • Journal Article • DOI:10.1103/PHYSREVB.22.2767

Ab initio studies of the x-ray absorption edge in copper complexes. I. Atomic Cu 2 + and Cu(ii) Cl 2 — Source link

Raymond A. Bair, William A. Goddard

Institutions: California Institute of Technology

Published on: 15 Sep 1980 - Physical Review B (American Physical Society)

Topics: Absorption (logic)

Ab initio studies of the x-ray absorption edge in copper complexes. I. Atomic Cu^{2+} and Cu(II)Cl_2

Raymond A. Bair and William A. Goddard III
Arthur Amos Noyes Laboratory of Chemical Physics, California Institute of Technology, Pasadena, California 91125
(Received 22 January 1980)

As a first step in the study of the structure at x-ray absorption edges, we have examined the discrete transitions corresponding to the atomic $1s \rightarrow 3d$, $4s$, $4p$, $5s$, and $5p$ transitions and the corresponding shakeup processes for Cu atom and for a Cu(II) model system, $CuCl_2$. For $CuCl_2$ the lowest strong transitions have the character $1s \rightarrow 4p$ ($f = 0.001\,33$). About 7.5 eV lower is a group of transitions involving $1s \rightarrow 4p$ simultaneous with ligand-to-metal shakedown. About 18.7 eV below the main peak is a weak (65 times weaker) quadrupole-allowed transition corresponding to $1s \rightarrow 3d$ (i.e., $1s^2 3d^9 \rightarrow 1s^1 3d^{10}$). These results are in agreement with typical assignments of x-ray absorption spectra of Cu(II) systems except that the middle transition is usually assigned as $1s \rightarrow 4s$, whereas we find this transition to be $1s \rightarrow 4p$ plus shakedown. (Transitions of the character $1s \rightarrow 4s$ are calculated but have intensities far too low to have been observed.)

I. INTRODUCTION

With the availability of synchrotron radiation sources, the analysis of extended x-ray-absorption fine structure (EXAFS) has developed into a powerful tool for the study of the local environment of transition metals in enzyme systems,[1–5] on surfaces,[6] in solution,[7] and in crystalline complexes.[8] EXAFS spectroscopy allows the study of the coordination of a specific element. The modulation of the characteristic absorption provides specific information about the chemical environment, including the species, number, and distances of neighboring atoms. However, current methods of analysis of the fine structure do not provide information about bond angles.

Recently, EXAFS techniques have been used in studies of copper coordination spheres in several biologically important metalloproteins (cytochrome-*c* oxidase,[3] azurin,[4] superoxide dismutase,[5] and others) not generally amenable to x-ray crystallographic techniques. In addition, the analysis of the structure in the x-ray absorption edge (x-ray absorption-edge spectroscopy, XAES) provides information about the oxidation state of the metal and about the electronic structure of the ligands bound to the metal.[2,9,10] A more detailed theoretical understanding of these absorption-edge phenomena would provide the experimentalist with another useful tool in the analysis of molecular structure. The absorption edge often shows shoulders (Fig. 1) which correspond to $1s \rightarrow$ valence and $1s \rightarrow$ empty bound-state transitions on the metal. Previously, the analysis of these particular features has been based on state splittings of atomic spectroscopy,[9] although significant changes are expected in these states upon molecule formation.

In this paper we have carried out *ab initio* calculations on a model copper complex in order to eluci-

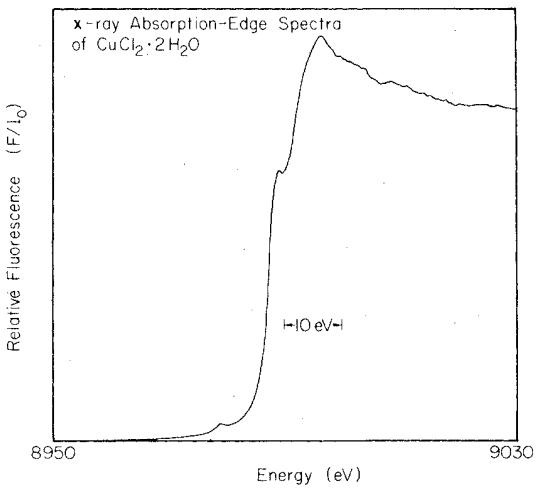

FIG. 1. EXAFS spectrum of crystalline $CuCl_2 \cdot 2H_2O$, courtesy of Chan *et al.* (Ref. 2). Here each copper atom [Cu(II)] is octahedrally coordinated to four chlorines and two water molecules. This spectrum shows the three edge features typical of Cu(II) complexes.

date the nature of the transitions involved in the absorption edge for a molecular system. We report calculations on excited states of the $CuCl_2$ molecule and Cu atom involving excitations from the $1s$ orbital of Cu, into the bound valence and virtual orbitals. $CuCl_2$ is a simple model that adequately demonstrates many of the features of the x-ray absorption edge to be found in other Cu(II) complexes. It has been observed in the gas phase[11] (although no EXAFS spectra have been reported). Details about the calculational methods used are in Sec. V.

II. DISCUSSION

A. Copper atom

We performed *ab initio* calculations involving excitations from the Cu $1s$ orbital as a benchmark with two purposes in mind. First, it has been proposed[9] that the splittings of the $1s$ hole states of copper should be very similar to the splittings of the corresponding valence states of Zn atom (with the $1s$ doubly occupied). We wished to test this hypothesis; and second, knowledge of the *ab initio* atomic splittings will be useful when considering the $CuCl_2$ complex in Sec. III.

Since Cu(II) complexes may often be considered as having $(3d)^9$ occupation on the metal, we calculated the $1s$ excitations of the corresponding Cu^{2+} ion. The ground state of Cu^{2+} is ^2D with a single $3d$ hole and no $4s$ electrons. The $1s$ excitations of Cu^{2+} are compared with the corresponding valence and Rydberg states of Zn^{2+} in Fig. 2. Here we have chosen the $(1s)^1(3d)^{10}$ state of Cu^{2+} and the $(1s)^2(3d)^{10}$ ground state of Zn^{2+} as the zero in energy (the remaining $n=2$ and $n=3$ orbitals are filled). (To have consistent valence exchange interactions, we have compared the quartet excited states of Cu^{2+} with the triplet states of Zn^{2+}.) The self-consistent-field (SCF) calculations are in good agreement with the five experimentally known Zn^{2+} states. Considering the large excitation energies involved (10 to 40 eV above the ground state), the errors in our calculation (0.2 to 0.8 eV) are of minor importance.

Table I lists the results of calculations of the allowed Cu^{2+} excitations from the $1s$ orbital to doublet excited states, along with the calculated oscillator strengths. Only the allowed electric dipole and electric quadrupole transitions are listed (there are no allowed magnetic dipole transitions from the $1s$ orbital). From these data we see that the lowest allowed electric dipole transition ($1s \rightarrow 4p$) is 87 times stronger than the allowed quadrupole transition ($1s \rightarrow 3d$).

The splittings of the atomic Cu^{2+} ($1s$) excitations are indeed quite similar to the splittings of the

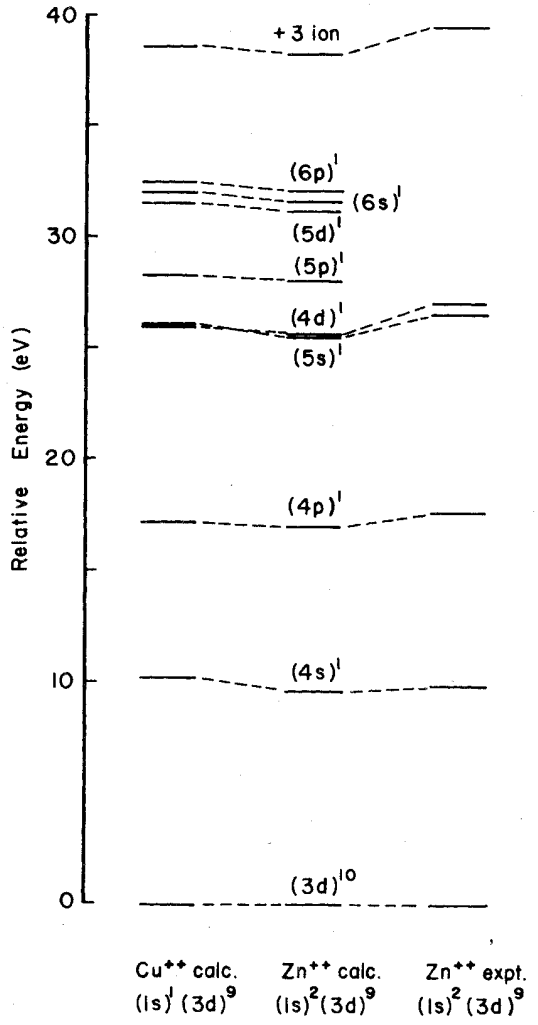

FIG. 2. *K*-shell quartet excited states calculated for Cu^{2+} as compared with the calculated and experimental (Ref. 12) triplet valence excited states of Zn^{2+}. In each case the remaining $n=2$ and $n=3$ levels are filled. The SCF calculations are described in Sec. V. The energies are the average of the five $3d$ hole states. Likewise, the experimental atomic states were averaged within each electronic configuration.

valence electronic states of Zn^{2+}. In this sense the previous efforts[2,9] to analyze the absorption-edge features based on those $Z=N+1$ atomic spectra cannot be faulted. However, in Sec. I, we will examine the differences in these states in a sample Cu(II) complex. There it will be shown that the ligands have a significant influence and introduce additional satellite transitions, not possible for the atomic ion. Also, in complexes, the charge on the Cu will tend to be closer to neutral, compressing the spectrum of Rydberg states into a smaller energy range.

TABLE I. Low-lying electric dipole and quadrupole K-shell transitions of Cu^{2+} from SCF calculations.

Term symbol	Electron configuration[a]	Transition	Excitation energy (eV)	Oscillator strength (f)
^2D	$(1s)^2(3d)^9$		−8894.14	ground state
^2S	$(1s)^1(3d)^{10}$	$1s \rightarrow 3d$	0.0[b]	1.93×10^{-5}
^2D	$(1s)^1(3d)^9(4s)^1$	$1s \rightarrow 4s$	10.43	0.0[c]
^2D			10.83	0.0[c]
^2P	$(1s)^1(3d)^9(4p)^1$	$1s \rightarrow 4p$	16.85	0.003 55
^2F			17.18	0.005 83
^2F			17.38	0.005 94
^2P			17.86	0.001 49
			$1s \rightarrow 4p$ Total	0.016 81
^2P	$(1s)^1(3d)^9(5p)^1$	$1s \rightarrow 5p$	28.18	0.001 30
^2F			28.29	0.002 22
^2F			28.34	0.002 02
^2P			28.48	0.000 52
			$1s \rightarrow 5p$ Total	0.006 06
^2P	$(1s)^1(3d)^9(6p)^1$	$1s \rightarrow 6p$	32.39	0.000 77
^2F			32.45	0.001 65
^2F			32.46	0.000 76
^2P			32.54	0.000 27
			$1s \rightarrow 76p$ Total	0.003 45

[a]The remaining orbitals of the $n=2$ and $n=3$ shells are filled.
[b]We choose the d^{10} excited state as the zero of energy.
[c]The transition to the $4s$ excited state is included as a reference; it is forbidden.

B. $CuCl_2$

In this section we will describe the $1s$ excitations in the $CuCl_2$ system. Although this is a small complex with only two ligands, many of the ideas developed from the $CuCl_2$ calculations have direct application to larger transition-metal complexes with more ligands and different metal centers. The ground state of $CuCl_2$ is $^2\Sigma_g^+$ and may be qualitatively considered as two chloride ions (Cl^{-1}) along the z axis bound to a d^9 Cu^{2+} atom (with the d_{z^2} orbital singly occupied). In this discussion we will be concerned with the occupation of the Cu $1s$ and $3d_{z^2}$ orbitals as well as the highest occupied Cl ligand orbital of each symmetry. We will also be exciting into some of the unoccupied diffuse $CuCl_2$ orbitals (e.g., the $4s$- and $4p$-like molecular orbitals). Hence, for the benefit of the reader we have constructed Table II which gives the occupation of these important orbitals in the ground state of $CuCl_2$ and in the various classes of excited states of interest.

Our calculated excitation energies for the lowest K-shell excitations of $CuCl_2$ are listed in Table III. The calculated oscillator strengths of the allowed transitions are also shown in this table. As expected, the lowest energy transition corresponds to exciting the $1s$ electron into the $3d$ hole in the Cu. This transition is electric dipole forbidden but quadrupole allowed. The oscillator strength[13] is small ($f = 1.92 \times 10^{-5}$), and almost identical to the value for the atomic ion. Experimentally, high-resolution x-ray absorption-edge spectra of Mn, Fe, Co, Ni, and Cu complexes all show a small feature on the low-energy side of the main absorption edge (e.g., see Fig. 1).[2,9,14] This has been previously identified as the $1s \rightarrow 3d$(-hole) transition. In fact, for $KFeF_3$ and K_2NaF_6 crystals, the EXAFS spectra of Shulman and co-workers[9] show both the $1s \rightarrow 3d_{t_2}$ and $1s \rightarrow 3d_e$ absorption features. The transition energies differ by approximately the value of ten Dq for these complexes, as expected. It has been proposed that vibronic coupling serves to increase the intensity of these $(1s)^2d^n \rightarrow (1s)^1d^{n+1}$ transitions by mixing p character into the upper states. This would introduce an electric dipole component into the transition and increase its intensity. However, we find that the electric quadrupole transition moment calculated for $CuCl_2$ leads to an intensity comparable to the ob-

TABLE II. Occupation of the $CuCl_2$ orbitals in selected states. The remaining $n=2$ and $n=3$ orbitals on Cu are doubly occupied, as are the $n=1$ and $n=2$ orbitals on Cl. There are two doublet states arising from each three open-shell configuration.

State	Description	Orbitals localized on Cu			Highest Cl $3p$ orbitals			
		$1s$	$3d_{z^2}$	Rydberg	σ_g^+	σ_u^+	π_g	π_u
$^2\Sigma_g^+$	ground state	2	1	0	2	2	4	4
$^2\Sigma_g^+$	$1s \rightarrow 3d_{z^2}$	1	2	0	2	2	4	4
Shakedown excitation	$1s \rightarrow$ Rydberg plus $\sigma_g^+ \rightarrow 3d_{z^2}$	1	2	1	1	2	4	4
Direct excitation	$1s \rightarrow$ Rydberg	1	1	1	2	2	4	4

served values without vibrational enhancement (of course, such enhancement may also be present). We will often use this transition (the lowest-energy peak) as the relative zero of energy.

In the range of 8 to 12 eV (Table III) above the first $^2\Sigma_g^+$ excited state, there are four sets of states that can be termed shakedown transitions. To explain, we will first consider the ionization of $CuCl_2$ from the Cu $1s$ level. Our calculations show that when the $1s$ electron is removed and the wave function permitted to relax, the ground state changes from d^9 in $CuCl_2$ to d^{10} in $CuCl_2^+$. The electron that fills the d_{z^2} hole can come from any one of the highest occupied ligand orbitals. Table IV lists the energies of the states formed by ionization directly from the Cu $1s$ and also the shakedown ionizations from the highest ligand orbitals of each symmetry. Note that all four of the shakedown d^{10} ions are 6 to 8 eV lower than the d^9 ion. This shakedown process is similar to a ligand-to-metal charge transfer, though the net charge on the Cu does not change appreciably (since the other valence orbitals polarize to neutralize any charge separation). These $CuCl_2^+$ results suggest that a Cu $1s$-to-Rydberg transition plus a simultane-

TABLE III. Low-lying K-shell excited states of $CuCl_2$ from configuration interaction calculations.

State	Description[a]	Excitation energy (eV)	Oscillator strength (f)
$^2\Sigma_g^+$	ground state	−8891.31	...
$^2\Sigma_g^+$	Cu $1s \rightarrow 3d_{z^2}$	0.0[b]	1.92×10^{-5}
$^2\Sigma_g^+$	Cu $1s \rightarrow 4s$ + shakedown	7.95[c]	0.0
		10.09[c]	0.0
$^2\Pi_u$	Cu $1s \rightarrow 4p_\pi$ + shakedown	9.88	0.000 204
		10.59	0.000 071
$^2\Sigma_u^+$	Cu $1s \rightarrow 4p_\sigma$ + shakedown	12.15	1.37×10^{-6}
		12.20	7.70×10^{-7}
$^2\Sigma_g^+$	Cu $1s \rightarrow 4s$	13.32[c]	0.0
		14.70[c]	0.0
$^2\Pi_u$	Cu $1s \rightarrow 4p_\pi$	16.42	0.000 595
		16.50	0.000 721
$^2\Sigma_u^+$	Cu $1s \rightarrow 4p_\sigma$	20.70	9.64×10^{-6}
		21.07	8.80×10^{-7}

[a]By $4p_\sigma$ and $4p_\pi$ we mean the low-lying Rydberg-like molecular orbitals of σ_g^+ and π_u symmetry that resemble the Cu $4p$ functions.

[b]We choose the d^{10} excited state as the zero of energy.

[c]The excitation energies into the $4s$-like molecular orbital are from SCF calculations.

ous shakedown in the form of a ligand-to-metal charge transfer should produce states lower in energy than the direct Cu 1*s*-to-Rydberg transition, without the shakedown. Our results (in Table III) confirm this analysis. There is a 5 to 9 eV separation between the corresponding direct and shakedown states in $CuCl_2$. This separation corresponds closely to the splitting (6 to 8 eV) of the d^9 and d^{10} ions of Table IV.

To illustrate, we will explicitly consider one set of the shakedown excitations—those where the highest σ_g ligand orbital is singly occupied. This σ_g ligand orbital has the same symmetry as the Cu d_{z^2} orbital, so in this case we can consider that the d_{z^2} hole, which was localized on the Cu in the ground state has readjusted to become localized on the chlorines in the excited state. The lowest such shakedown state involves the Cu 1*s* excitation to a Cu 4*s*-like orbital. This 4*s* orbital is plotted in Fig. 3 along with the atomic 4*s* orbital for Cu^{2+}. We can see that the molecular orbital (of σ_g^+ symmetry) is more diffuse than the atomic orbital and has a significant amount of ligand character. This transition leads to two $^2\Sigma_g^+$ states, differing in the spin coupling of the three open-shell electrons. (These are separated by approximately twice the Cu $3d_{z^2}$-4*s* exchange interaction.) Both components are symmetry-forbidden, so that this 1*s*-to-4*s* shakedown transition is not to be observed.

The next higher shakedown state (with σ_g^+ ligand hole) involves the 1*s*-to-$4p_\pi$ transition ($4p_x$ or $4p_y$). In this case, the $4p_\pi$ orbitals are slightly larger than the atomic 4*p* orbitals (see Fig. 3). This transition to the $^2\Pi_u$ excited state is symmetry allowed, though we find that it is not very strong ($f = 2.7 \times 10^{-4}$, Table III). The reason it has a small oscillator strength lies in the nature of the shakedown process. Qualitatively, the transition moment for all these shakedown transitions varies as the transition moment from the 1*s* to the virtual orbital ($4p_\pi$ in this case) *times* the overlap of the d_{z^2} orbital of the ground-state wave function with the singly occupied ligand orbital in the excited state[15] (highest σ_g^+ in this case). For this reason the transition moments for the shakedown transitions are smaller than the direct transitions by a factor of this overlap. Also, only shakedown transitions involving the σ_g^+ ligand orbitals will have any intensity since only those ligand orbitals can overlap with the Cu d_{z^2} orbital. Note that the *ground-state* $3d_{z^2}$ orbital can overlap the *excited state* σ_g^+ orbital since the excited-state wave function is allowed to relax (self-consistently). The orbitals change shape in the excited state, leading to an overlap of ~0.37 in this case (the total many-electron wave functions do not, of course, overlap). The amplitudes of these two orbitals are plotted in Fig. 4 (*a* is d_{z^2}, *b* is ligand σ_g).

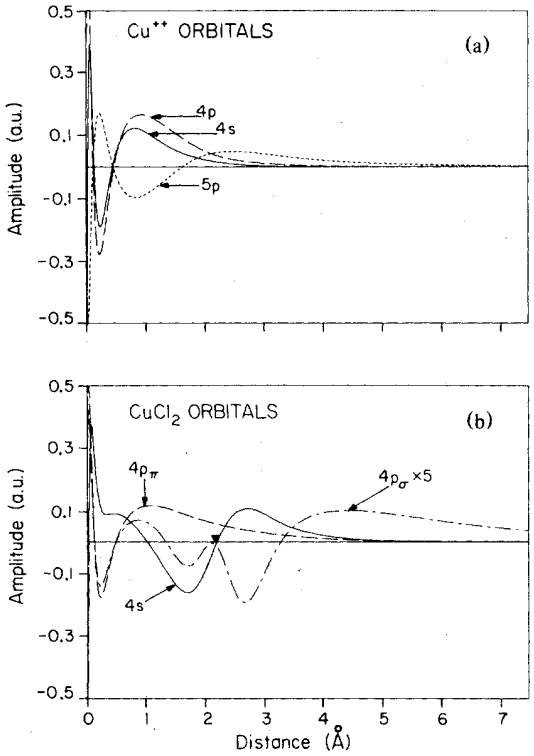

FIG. 3. Orbital amplitudes as a function of distance from the Cu for the excited state 4*s*, 4*p*, and 5*p* orbitals of Cu^{2+} (a) and the 4*s*, $4p_\pi$, and $4p_\sigma$ orbitals of $CuCl_2$ (b). For $CuCl_2$, the 4*s* and $4p_\sigma$ amplitudes are shown along the molecular axis, while the $4p_\pi$ amplitude is perpendicular to this axis.

TABLE IV. Calculated *K*-shell ionization potentials of $CuCl_2$.

State	Ligand hole[a]	Ionization potential (eV)	Relative energy (eV)
$^3\Sigma_g^+$	Cu $3d_{z^2}$	8914.8	0
$^3\Sigma_g^+$	σ_g^+	8908.3	−6.5
$^3\Sigma_u^+$	σ_u^+	8907.9	−6.9
$^3\Pi_u$	π_u	8907.2	−7.6
$^3\Pi_g$	π_g	8906.9	−7.9

[a]In each case the ligand hole is the highest occupied molecular orbital of the indicated symmetry.

The next shakedown state in this series is to a Cu 5*s*-like orbital. It is also forbidden. At 1.9 eV above the excitation to the $4p_\pi$ states we find the transition to the $4p_z$. This $4p_z$ orbital, plotted in Fig. 3 together with the Cu^{2+} atomic orbital, is strongly affected by the proximity of the occupied Cl orbitals and has been pushed higher in energy. This leads to the 1.9 eV splitting, which has implications for four- and

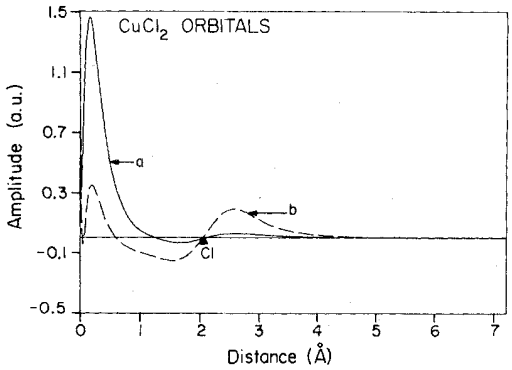

FIG. 4. Orbital amplitudes as a function of distance along the $CuCl_2$ molecular axis. The solid line (a) is the amplitude of the singly occupied $3d_{z^2}$ orbital in the ground state. The dashed line (b) is the amplitude of the singly occupied ligand σ_g^+ orbital in the shakedown excited states. Note the overlap of these two orbitals.

six-coordinated complexes, as discussed later. Also, the more diffuse nature of the $4p_z$ orbital reduces the strength of this transition, relative to the corresponding $4p_\pi$ state.

We assign these ($1s \rightarrow 4p$) shakedown transitions (both $4p_\pi$ and $4p_\sigma$) to the absorption peak commonly identified as the $1s \rightarrow$"$4s$" direct transition (see Fig. 1). There are two factors to consider in reassigning this absorption-edge feature. The first is intensity. We find that the $1s$-to-$4p$ shakedown is 80% weaker than the $1s$-to-$4p$ direct transition, whereas the $1s$-to-$4s$ direct transition is symmetry forbidden. Even in complexes with low symmetry, considerable p character would have to be built into the lowest unoccupied molecular orbital (about 14%) for the intensity to rival that of our $1s \rightarrow 4p$ shakedown transition. The second factor is energy position. We find that although the $1s$-$4s$ transition is ~6.6 eV below $1s \rightarrow 4p$ in Cu^{2+} ions, it is displaced in $CuCl_2$ to be only 2.2 eV below $1s \rightarrow 4p$ (due to interactions of the excited orbital with the ligands). We find the $1s \rightarrow 4p$ shakedown transition at ~7.5 eV below the $1s \rightarrow 4p$ direct; about the same location as observed experimentally. Empirical evidence in favor of our reassignment can be obtained from studies of the first-row transition-metal fluorides.[9] Shulman *et al.*[9] find that the difference in energy between the $1s$-to-"$4s$" ($1s$-to-$4p$ plus shakedown in our assignment) and $1s$-to-$4p$ is nearly constant for the divalent elements Mn(II) through Ni(II). This result is consistent with either assignment. However, the $1s$-to-$4s$ assignment predicts a large (10 eV) "$4s$"-$4p$ splitting for the corresponding Fe(II) complex in the next higher oxidation state. Here our assignment would predict a smaller increase in the splitting of the $1s$-to-$4p$ plus shakeup, versus the $1s$-to-$4p$ direct states. This splitting is just the difference in energy between the $L_e^4 d^n$ configuration (where L_e is the highest ligand e level) and the $L_e^3 d^{n+1}$ configuration resulting from the shakedown process, which is expected to be approximately constant with changes in oxidation state of the metal. Thus the 7-eV splitting observed[9] for K_2NaFeF_6 is more consistent with our assignment. Similar arguments apply to the analysis of the higher states in this series. The transitions to s- or d-like unoccupied orbitals are forbidden and those to p-like orbitals are allowed.

Shakedowns from the other three high ligand orbitals (see Table II) give the same ordering of states in the same energy range (Table V) and will not be discussed separately. However, these transitions are symmetry-forbidden from the ground state.

Finally, at 13 eV above the lowest excited state ($^2\Sigma_g^+$) we calculate the first direct transition from the Cu $1s$ to the $4s$-like unoccupied molecular orbital. This transition is forbidden. The next state, a transition to the $4p_\pi$ is allowed and occurs 6.2 eV above the corresponding shakedown state. The $4p_\sigma(4p_z)$ level occurs 4.4 eV above the $4p_\pi$ level. This splitting is caused by the axial ligands, and would be much smaller in tetrahedrally or octahedrally coordinated Cu(II) complexes. The $5p_\pi$ states occur 3.1 eV above the $n=4$ levels and are expected to be much weaker, since the intensity of this transition falls off

TABLE V. Calculated K-shell excited states involving shakedown for $CuCl_2$.

Rydberg orbital occupied in excited state	Excited state energy (eV) for each ligand hole[a] σ_g^+	σ_u^+	π_g	π_u
$4s$	7.95, 10.09	7.12, 9.69	6.62, 6.80	6.90, 7.15
$4p_\pi$	9.88, 10.59	9.62, 9.73	8.26 – 9.56	8.52 – 9.74
$4p_\sigma$	12.15, 12.20	11.60, 11.67	10.68, 10.74	10.98, 11.04

[a]Using the $(1s)^1(3d)^{10}$ state as the zero of energy.

rapidly as the size of the np orbital increases. Similarly, the $5p_\sigma$ state is 1 eV above the $4p_\sigma$ state, though the $5p_\sigma$-like orbital is so diffuse that our description of this particular state is less accurate than the others.

We find that the oscillator strength of the atomic $1s$-to-$4p$ transitions is decreased by a factor of 12 in $CuCl_2$ (Tables I and III). The molecular $4p$ orbitals are more diffuse than atomic $4p$ orbitals and indeed are comparable in size to atomic $5p$ orbitals. Since the $1s$-to-$5p$ atomic transition is a factor of 2.8 weaker than $1s$-to-$4p$, this size difference could account for a major part of the decrease in intensity in the molecular transition. In addition, the $CuCl_2$ excited $4p$ orbital has character on the ligands, further decreasing the intensity (for the transition from Cu $1s$).

On the other hand, the direct transitions are 4.8 times as strong as the shakedown transitions. From the overlap of the ground-state $3d_{Z^2}$ orbital and the shakedown excited-state open-shell ligand Σ orbital ($S=0.37$), we would expect a factor of 7.1. Thus, qualitatively, the transition moment from the $1s$ to the $4p$ is similiar, and the difference in intensity arises primarily from the overlap term introduced by the shakedown.

In conclusion, our $CuCl_2$ calculations allow us to make assignments of the common three absorption-edge features of Cu(II) EXAFS spectra. The lowest energy transition is a weak quadrupole-allowed Cu $1s \rightarrow 3d$ transition. The next absorption corresponds to the dipole-allowed $1s$-to-$4p$ plus ligand-to-metal shakedown, and the most intense peak is the direct $1s$-to-$4p$ transition. It is important to note that in each case the spectral feature has been assigned to an allowed transition. This differentiates our assignment of the middle peak from previous work and has implications about the x-ray absorption-edge spectroscopy of the transition metals, as illustrated in Sec. III.

III. APPLICATIONS TO OTHER SYSTEMS

In this section we will consider the application of our ideas about Cu(II) systems to the other transition metals in the Cu row. Also, we will briefly discuss the effects of mixed ligands and low symmetry. First we examine the divalent transition-metal fluorides, KMF_3, where the metal occupies an octahedral site.[16]

The EXAFS spectra are available[9] for Mn(II) through Zn(II), with the exception of Cu. Of these, Mn(II) through Cu(II) all have an unfilled e_g-type metal d orbital. Thus we expect to observe at least three transitions on the absorption edge. At low energy there is an electric quadrupole-allowed $1s \rightarrow 3d$ transition with low intensity. In the metals with an unoccupied t_2-type d orbital [as in V(II) through Co(II)], the $1s \rightarrow 3d$ transition may be split into $1s \rightarrow 3d_e$ and $1s \rightarrow 3d_{t_2}$ components. The energy separation is approximately ten Dq for the corresponding complex containing the metal of the next higher atomic number.[17] Then, about 5–7 eV higher there is a shoulder,[9] representing a $1s \rightarrow 4p$ plus shakedown transition of intermediate intensity. Finally, at the apex of the edge, there is a strong $1s \rightarrow 4p$ transition.

For Zn(II), there are no d holes so we do not expect either $1s \rightarrow 3d$ or shakedown transitions. It would then be consistent to assign the lowest energy feature to the $1s \rightarrow 4p$. However, two peaks are observed at the top of the absorption edge.[9] Even assuming strong vibrational coupling, the lower energy peak appears much stronger than would be reasonable for a $1s \rightarrow 4s$ transition. Therefore we tentatively reassign the *lower* energy peak to the $1s \rightarrow 4p$, which should be a strong transition. There are several possibilities for the origin of the higher-energy transitions, including (i) a $1s \rightarrow 4p$ plus shakeup state (where this shakeup would involve a transition from a $3d$ orbital to a virtual orbital of the same symmetry) or (ii) the $1s \rightarrow 5p$ transition.

Now, considering the first part of the row [Ti(II) through Cr(II)], we expect the trifluoride crystals to have qualitatively the same absorption-edge features as for Mn(II) through Cu(II), with one notable exception. This exception is Cr(II), which is formally d^4. For this metal the ligand-to-metal shakedown has two nondegenerate components. Since the Cr(II) $3d\ e_g$ level has only one electron, the electron that comes from the ligand e_g orbital into the $3d\ e_g$ level may be either singlet or triplet coupled to the single $3d$ electron already there. Both of these $3d$ spin configurations may be coupled to the remaining $1s$ and $4p$ singly occupied orbitals to produce an overall quintet excited state. This splitting should be about twice the $3d$ exchange integral (for the excited state), around 1.2 to 1.9 eV. Thus, in the Cr(II) trihalide crystal, the EXAFS experiment is predicted to show two shakedown transitions. This experiment, if performed, may serve to differentiate our assignment of the second peak from the $1s \rightarrow 4s$ assignment made previously. The $1s \rightarrow 4s$ transition is also split into two components; however, the energy difference is only twice the $3d$-$4s$ exchange interaction, which is smaller, about 0.4 to 0.6 eV.

Now we consider the qualitative features of the edge spectra of mixed ligand complexes for the first transition series. Here, each chemically different ligand may give rise to a shakedown transition of a different energy. This transition can be described as a metal $1s \rightarrow 4p$ plus a ligand-to-metal charge transfer involving the ligand lone-pair Σ bonding to the metal and the metal-d orbital(s) oriented Σ to this ligand orbital. If there are several ligands of the same type, a particular shakedown transition may be enhanced. Of course this analysis applies best to ionic bonds.

Covalently bound ligands may have such satellite transitions that are actually higher in energy than the corresponding direct transition. In addition, the $4p$ virtual orbitals are not degenerate in complexes with low symmetry. In fact, our $CuCl_2$ calculations show a 2–4-eV splitting, probably an extreme. Because of this splitting, it may be possible to observe the components of both the $1s \rightarrow 4p$ shakedown and the $1s \rightarrow 4p$ direct transitions. This would provide some supportive information about bond angles and molecular symmetry. Along this vein, we have initiated calculations to compare square planar and tetrahedral conformations of a model Cu complex.

IV. SUMMARY

We have carried out *ab inito* self-consistent-field (SCF) and configuration interaction calculations on the $CuCl_2$ system and related our results to the K-edge x-ray absorption spectra of transition-metal complexes. The three common features on the K edge were described by our calculations. The assignment of the $1s \rightarrow 3d$ and $1s \rightarrow 4p$ transitions agrees with previous assignments. We have reassigned the $1s \rightarrow$ "$4s$" transition as an allowed $1s$-to-$4p$ transition with a concurrent ligand-to-metal shakedown. This shakedown involves the ligand orbital sigma to the metal and a d-hole sigma to the ligand.

V. DETAILS OF THE CALCULATIONS

A. Basis set

All of the calculations used the Cu (^2S) Gaussian basis set of Wachters[18] with the first six s functions, the first five p functions, and the first four d functions contracted to form a single final s-, p-, and d-basis function, respectively. The remaining functions were left uncontracted. This contraction system allows more flexibility in the Cu core functions than the usual double ζ contraction of Wachters functions. We felt that this extra flexibility was necessary to adequately describe the core electronic relaxation after $1s$ excitation. In addition, we replaced the two $4s$ functions of the Wachters basis with four Gaussians having exponents of 0.3324, 0.1108, 0.031 66, and 0.008 442 in order to also describe both $4s$ and $5s$-like orbitals. Similarly, we replaced the outer two $4p$ functions with four Gaussians (0.2099, 0.059 98, 0.017 14, and 0.004 570) in order to describe both $4p$- and $5p$-like orbitals. We also added two diffuse d functions with Gaussian exponents of 0.1168 and 0.0329. All together, this gives a basis size of 62 final functions on the metal and more than double ζ quality (only the innermost $1s$, $2p$, and $3d$ functions contracted). For the Cl atoms in the $CuCl_2$ calculations, we used an effective potential[19] to replace the Ne core of Cl. This potential reduces the Cl basis set to those functions describing the valence orbitals. This double ζ Cl basis was contracted[20] to a minimum basis set by explicit optimization of the contraction for $CuCl_2$. Thus, our final CI basis consisted of four functions, with the contraction optimized for $CuCl_2$. The CuCl bond distance of 2.17 Å was taken from SCF calculations[21] (double ζ basis) on $CuCl_2$. (The experimental bond distance is not known.)

B. Wave functions

To calculate the atomic excitation energies, we carried out SCF calculations using the fully-optimized open-shell Hartree-Fock wave functions. For the atomic wave functions with $(3d)^9$ occupation, we solve for an average d^9 state in the same manner as reported previously.[22] Here the variational Hamiltonian (Fock operator) was derived from the average energy of the five possible d holes. Some of the excited-state atomic wave functions were constructed using the improved virtual orbital (IVO) method.[23] In general, all the Rydberg states could be obtained from a single SCF calculation for the lowest Rydberg state and a set of IVO's providing an orthogonal set of Rydberg orbitals. We checked these IVO results by performing additional SCF calculations on the Cu^{2+} ion. The largest error for any state in Fig. 2 was 0.06 eV. The Rydberg states were calculated as high-spin (quartets) and we performed a small configuration interaction (CI) calculation to obtain the energies for the low-spin (doublet) states. Indeed, the manifold of states arising from the quartet SCF and IVO calculations is energetically almost the same (0.03 eV difference) as the average of the corresponding doublet states from the CI, thus justifying this straightforward approach. (This result is expected since the exchange interactions between the $1s$ and open-shell valence orbitals are small.) The atomic oscillator strengths were determined by calculating the (length-form) transition moments between the ground- and excited-state SCF wave functions, allowing electronic relaxation,[24] and including the correct excited-state spin coupling as optimized in the CI. Again, since the excited doublet and quartet states are so close in energy, we could use the SCF orbitals from the quartet state to describe the doublet states.

For the $CuCl_2$ complex, the same kind of open-shell SCF calculations were carried out, but without averaging the $3d$ hole. Here we found an accurate, simple method for obtaining the spectrum of excited states for the direct and shakedown transitions. For those states with an occupied Rydberg orbital, we removed the Rydberg electron and calculated the corresponding positive ion wave function by SCF methods.

TABLE VI. Comparison of excitation energies and oscillator strengths of $CuCl_2$ transitions calculated by SCF and CI methods.

State	SCF excitation energy (eV)	SCF oscillator strength (f)	CI excitation energy (eV)	CI oscillator strength (f)
$^2\Sigma_g^+$[a]	0.0	1.92×10^{-5}	0.0	1.92×10^{-5}
$^2\Pi_u$	10.03	1.28×10^{-4}	9.88	2.04×10^{-4}
	11.04	3.67×10^{-5}	10.59	7.13×10^{-5}
$^2\Sigma_u^+$	12.47	2.10×10^{-6}	12.15	1.37×10^{-6}
	12.55	1.09×10^{-9}	12.20	2.70×10^{-7}
$^2\Pi_u$	15.74	5.35×10^{-4}	16.42	5.95×10^{-4}
	15.88	2.79×10^{-4}	16.50	7.21×10^{-4}
$^2\Sigma_u^+$	18.91	1.85×10^{-5}	20.70	9.64×10^{-6}
	18.95	2.05×10^{-7}	21.07	8.80×10^{-7}

[a]This is the $Cu(1s)^1(3d)^{10}$ excited state.

Then we froze the occupied orbitals, replaced the Rydberg electron, and calculated the spectrum of orthogonal Rydberg orbitals. These results agreed within 0.007 eV of the fully relaxed SCF results for the several cases we tested. Again, as for the atom, we obtained the Rydberg states as quartets, and performed a small CI to get the doublet energies. The oscillator strengths were calculated by two different methods. First we calculated the moments between the ground- and excited-state SCF wave functions, allowing electronic relaxation and including the correct excited-state spin coupling for the three open-shell electrons (as we did for Cu^{2+}). The second method used the entire set of occupied orbitals from the ground and excited state in a larger CI. This orbital set included the 22 orbitals of the ground-state SCF wave functions, the 23 orbitals of the $(1s)^1(4p_x)^1$ plus shakedown excited state, and the $4p_z$ virtual orbital (all orthogonalized). The CI configuration list included the ground-state configuration, the four excited-state configurations (shakedown and direct to $4p_x$ and $4p_z$), and all single excitations from these four configurations requiring that the $1s$ orbital be singly occupied. This configuration list was adequate to describe the ground state, the $1s\rightarrow3d$ transition, and the $1s\rightarrow4p$ transitions (both shakedown and direct). The oscillator strengths were then calculated for these states of the CI. The results for both methods are presented in Table VI. This table shows that both approaches produce similar oscillator strengths. The agreement for the lower energy excited states is much better than for the higher ones. However, our aim was to determine the relative strength of these transitions, which we accomplished with a set of simple and consistent wave functions. Certainly this purpose was achieved, although in an absolute sense, oscillator strengths often vary (systematically) from the true value by a factor of 2 to 3 for such wave functions.

ACKNOWLEDGMENTS

One of the authors (R.A.B.) gratefully acknowledges support provided by a traineeship from the National Institutes of Health. Computing assistance was obtained from the Health Sciences Computing Facility of the University of California, Los Angeles, supported by the National Institutes of Health Research Resources Grant No. RR-3. This work was partially supported by NIH Research Grant No. GM-23971 from the National Institute of General Medical Sciences. Some of the calculations were carried out on the Dreyfus-NSF Chemistry Department DEC VAX 11/780 Computer, funded by grants from the Camille and Henry Dreyfus Foundation and from the NSF.

[1]R. G. Shulman, P. Eisenberger, and B. M. Kincaid, Annu. Rev. Biophys. Bioeng. 7, 559 (1978).
[2]S. I. Chan, V. W. Hu, and R. C. Gamble, J. Mol. Struct. 45, 239 (1978).
[3]V. W. Hu, S. I. Chan, and G. S. Brown, Proc. Natl. Acad. Sci. U.S.A. 74, 3821 (1977).
4 T. D. Tullius, P. Frank, and K. O. Hodgson, Proc. Natl. Acad. Sci. U.S.A. 75, 4069 (1978).
[5]W. E. Blumberg, J. Peisach, P. Eisenberger, and J. A. Fee, Biochemistry 17, 1842 (1978).
[6]J. H. Sinfelt, G. H. Via, and F. W. Lytle, J. Chem. Phys. 68, 2009 (1978).

[7]P. Eisenberger and B. M. Kincaid, Chem. Phys. Lett. 36, 134 (1977).
[8]G. Martens, P. Rabe, N. Schwentner, and A. Werner, Phys. Rev. B 17, 1481 (1978).
[9]R. G. Shulman, Y. Yafet, P. Eisenberger, and W. E. Blumberg, Proc. Natl. Acad. Sci. U.S.A. 73, 1384 (1976).
[10]F. A. Cotton and C. J. Ballhausen, J. Chem. Phys. 25, 617 (1956).
[11]C. W. DeKock and D. M. Gruen, J. Chem. Phys. 44, 4387 (1966); 49, 4521 (1968).
[12]C. E. Moore, *Atomic Energy Levels* (National Bureau of Standards Circular, Washington, D.C., 1971), Vol. II.
[13]For the electric quadrupole transitions, our oscillator strengths are: $f=\frac{2}{3}(\Delta E^3/C^2)M^2$, where M is the electric quadrupole transition moment between the two states of interest, c is the speed of light, and all quantities are in atomic units.
[14]R. G. Shulman, P. Eisenberger, B. K. Teo, B. M. Kincaid, and G. S. Brown, J. Mol. Biol. 124, 305 (1978).
[15]Not allowing the wave function to relax, the $1s$-to-$4p_z$ oscillator strength is

$$f=\tfrac{2}{3}\Delta E\langle\phi_{1s}|z|\phi_{4p}\rangle^2 ,$$

where ϕ_{1s} and ϕ_{4p_z} are the $1s$ and $4p_z$ orbitals of the frozen wave function. However, allowing the wave function to relax upon excitation introduces additional overlap factors. Most of the overlaps are very nearly 1, so they can be ignored here. However, in $CuCl_2$, the ground state is d^9 with the d_{Z^2} single occupied and the shakedown excited state is d^{10} with a singly occupied ligand orbital. This introduces a factor of the overlap of the ground state $3d_{Z^2}$ orbital, $\phi_{3d_{Z^2}}$ and the excited state ϕ'_L singly occupied ligand orbital. Thus, in this case,

$$f=\tfrac{2}{3}\Delta E(\langle\phi_{1s}|x|\phi'_{4p_z}\rangle\langle\phi_{3d_{Z^2}}|\phi'_L\rangle)^2 ,$$

where the overlap is $\sim$0.37.
[16]M. A. Hepworth, K. H. Jack, R. D. Peacock, and G. J. Westland, Acta Crystallogr. 10, 63 (1957).
[17]This splitting is shown clearly in the iron-fluoride spectra of Shulman and co-workers, Ref. 14.
[18]A. J. Wachters, J. Chem. Phys. 52, 1033 (1970).
[19]A. K. Rappé, T. A. Smedley, and W. A. Goddard III (unpublished).
[20]A. K. Rappé and W. A. Goddard III (unpublished).
[21]A. F. Voter and W. A. Goddard III (unpublished).
[22]R. A. Bair and W. A. Goddard III, J. Am. Chem. Soc. 99, 3505 (1977).
[23]W. J. Hunt and W. A. Goddard III, Chem. Phys. Lett. 3, 414 (1969).
[24]Our transition moments were calculated from separate SCF wave functions for the ground and excited states. This makes the actual evaluation of the moments much more difficult, but it is necessary since there is so much relaxation in the wave function in the $1s$ hole states.